Intrinsic optical signal imaging of neocortical seizures: the 'epileptic dip'

Sonya Bahar, Minah Suh, Mingrui Zhao and Theodore H. Schwartz

Department of Neurological Surgery, Weill-Cornell Medical College, New York Presbyterian Hospital, New York, New York, USA.

Correspondence and requests for reprints to Sonya Bahar, PhD, Center for Neurodynamics, Department of Physics and Astronomy, University of Missouri at St Louis, One University Boutevard, St Louis, MO 63121, USA
Tel: + 1 314 516 7150; fax: + 1 314 516 6152; e-mail: bahars@umsl.edu

Sponsorship: NIH/NINDS Grants K08NS43799 and R21NS044812 to T.H.S.

Received 6 December 2005; accepted 30 January 2006

Focal neocortical seizures, induced by injection of 4-aminopyridine, were imaged in the rat neocortex using the intrinsic optical signal, with incident light at various wavelengths. We observed focal, reproducible and prolonged reflectance drops following seizure onset, regardless of wavelength, in the ictal onset zone. A persistent drop in light reflectance with incident orange light, which corresponds to a decrease in oxygenated hemoglobin, was observed. We describe this phenomenon as an 'epileptic dip' as it is reminiscent of the 'initial dip' observed using the intrinsic optical signal, and also with blood oxygen level-dependent functional magnetic resonance imaging, after normal sensory processing, although with much longer duration. This persistent ictal ischemia was confirmed by direct measurement of tissue oxygenation using oxygen-sensitive electrodes. *NeuroReport* 17:499–503 © 2006 Lippincott Williams & Wilkins.

Keywords: 4-aminopyridine, epilepsy, hemoglobin oxygenation, initial dip, intrinsic optical signal, neocortex, optical imaging, rat

Introduction

The intrinsic optical signal (IOS) is a drop in light reflectance derived from activity-dependent physiological changes in neural tissue. At isosbestic wavelengths of hemoglobin, the IOS measures total hemoglobin (Hbt), which is directly proportional to cerebral blood volume (CBV) and cerebral blood flow (CBF), assuming constant red blood cell concentration [1–3]. At longer wavelengths (600–650 nm), the IOS reveals changes in hemoglobin oxygenation, as the absorption coefficient of deoxygenated hemoglobin (Hbr) is three times that of oxygenated hemoglobin (HbO_2) [4,5]. This signal is analogous to the blood oxygen level-dependent (BOLD) functional magnetic resonance (fMRI) signal [6]. At near-infrared wavelengths, a light-scattering component becomes significant [4,5].

The IOS has been used to image seizures *in vivo* in rat [7], ferret [8], and human [9]. More recently, Suh *et al*. [10], using wavelengths sensitive to Hbr, found a drop in light reflectance during interictal (between seizure) events, consistent with transient tissue ischemia. To determine whether ictal events similarly overwhelm the brain's ability to perfuse these highly metabolically active neurons, we imaged acute ictal events following focal injection of 4-aminopyridine (4-AP) into the rat neocortex *in vivo*, and confirmed our findings with direct measurement of tissue oxygenation.

Methods

Surgery

All procedures followed Cornell University Institutional Animal Care and Use Committee and Research Animal Resource Center guidelines. Male Sprague–Dawley rats (n=6; 250–375 g) were initially anesthetized with intraperitoneal ketamine (90 mg/kg) and xylazine (4.0 mg/kg) and sustained with urethane (1.25 gm/kg). Temperature was maintained at 37°C with a heating blanket (Harvard Apparatus, Holliston, Massachusetts, USA). Heart rate, O_2–saturation, and pCO_2 were monitored (SurgiVet, Waukesha, Wisconsin, USA); an electrocardiogram was recorded between leads attached to the right hindlimb and to the scalp, which was shaved. Rats were placed in a stereotactic frame, and the scalp was incised along the midline. The skull over one hemisphere, between lambda and bregma, was thinned with a dental drill. A $\sim$1 mm^2 hole was made in the thinned skull over the somatosensory cortex, and a slit was made in the dura.

Electrophysiology

A glass micropipette filled with 1% NaCl was positioned in the dural slit, $\sim$300 µm below the neocortical surface, for field potential recording. A second pipette, filled with 4-AP and attached to an oocyte injector (Drummond Scientific, Broomall, Pennsylvania, USA), was positioned $<$1 mm from the field potential electrode. The field potential and electrocardiogram were recorded with a (DBA-S system; World Precision Instruments (WPI), Sarasota, Florida, USA), digitized at 2000 Hz by a CED Power 1401 and recorded using Spike 2 software (Cambridge Electronic Design, Cambridge, UK). Electrographic seizures were induced by injecting 0.5 µl of 4-AP (25 mM in 1% NaCl) into cortical layers II–III [11].

Imaging and data acquisition

Agar (1.5% in 1% NaCl) and a glass cover slip were placed over the thinned skull, which was illuminated with a tungsten–halogen bulb. The light path passed through a filter at one of four wavelengths (546 ± 10, 605 ± 10, 630 ± 10, or 700 ± 10 nm) and was directed onto the cortex with two fiber optic light guides. A 10-bit CCD camera (Optical Imaging, Germantown, New York, USA), placed over a tandem configuration of two 50-mm lenses, was focused on the blood vessels on the cortical surface, and a raw image was taken to correlate the blood vessel pattern with subsequent images. The camera was then focused 500 μm below the cortical surface.

Images of a 9×7 mm area of the cortex were acquired every 600 ms using an Imager 3001 system (Optical Imaging Inc.) with 256×160 pixel resolution. A transistor-transistor logic pulse corresponding to the image acquisition time was recorded by the CED Power 1401 to correlate imaging with electrophysiology during offline analysis. Seizures were imaged at randomly selected wavelengths in order to avoid bias.

Image processing and data analysis

Reflectance changes were visualized by dividing images acquired during a seizure by a 'blank' image acquired before electrophysiological seizure onset, using custom software written in MATLAB (MATLAB; The Mathworks, Natick, Massachusetts, USA). The reflectance change at each time point was quantified as $-\Delta R/R$ (%) in a region of interest (ROI), where R is the mean pixel intensity within the ROI. Note that the negative sign means that a drop in reflectance will appear as a positive value of $-\Delta R/R$ (%); thus, positive values of $-\Delta R/R$ (%) correspond to increases in neural activity.

Raw (divided) images were spatially filtered using a moving average 5×5 pixel vector for smoothing. Filtered images were then used to calculate the spatial extent of the IOS, using normalized threshold analysis [12]. For a given set of images, the dynamic range of pixel intensities (minimum to maximum) was determined. Each pixel was evaluated to determine whether it was a given percentile of the dynamic range below the median; pixels satisfying this criterion were considered to belong to the 'seizure area'. The initial rate of seizure spread was determined from the slope of a linear fit to a plot of seizure radius vs. time during the first 3 s of activity, approximating the initial activated area as circular.

As light absorption by tissue varies with wavelength and depth, error can be introduced when wavelengths are compared. To adjust for this, many researchers perform a path-length correction by means of spectroscopic imaging [2,13,14]. Such corrections, however, are only possible when comparing 'identical' tissue responses, such as the response to multiple applications of identical sensory stimuli; here, each epileptic event is unique in spatial extent, electrophysiological progression, and duration, and such a direct spectroscopic comparison cannot be performed.

Direct measurement of tissue oxygenation

Tissue oxygenation was measured with a Clark-style polarographic oxygen microsensor (Unisense A/S, Aarhus, Denmark). Calibrations were performed at 37°C in saline

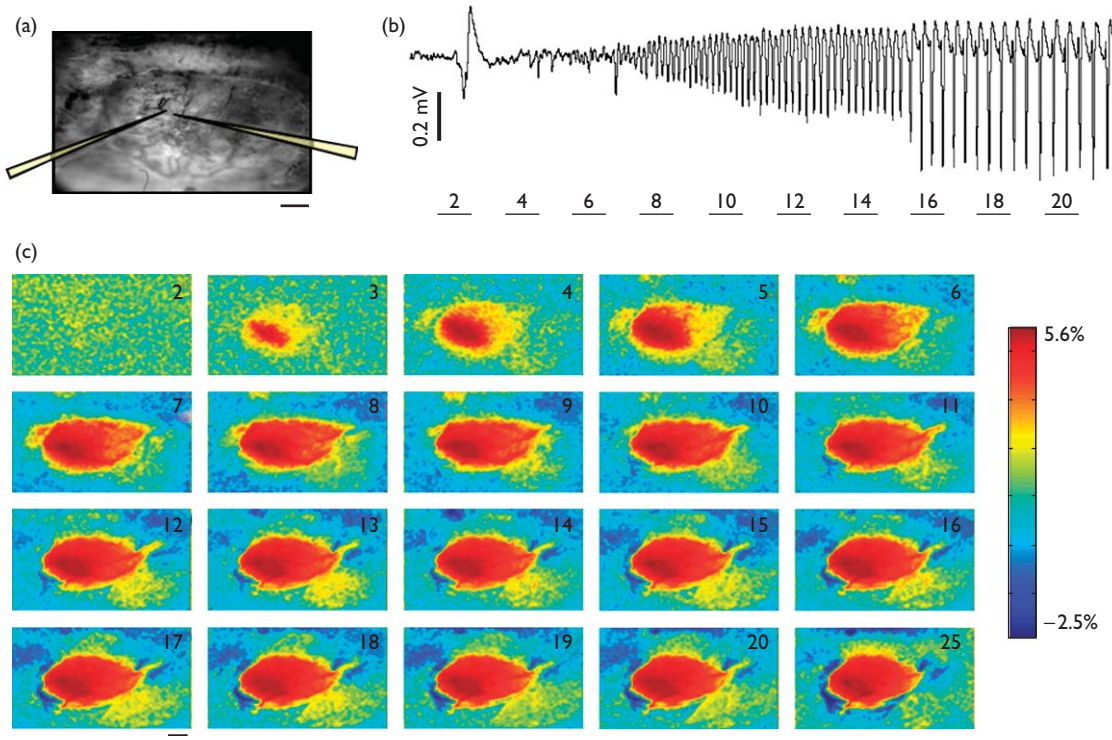

Fig. 1 (a) Image at 546 nm shows blood vessel pattern and position of 4-aminopyridine (left) and field potential (right) electrodes. Scale bar: 1 mm. (b) Field potential recording of seizure onset. Horizontal bars (0.6 s duration), represent alternate camera frames. (c) Images acquired at 605 nm, corresponding to frames indicated in (b). Frame 1 (not shown) was used as a denominator. Scale bar: 1 mm; color scale: $-\Delta R/R$ (%); red=maximum reflectance drop.

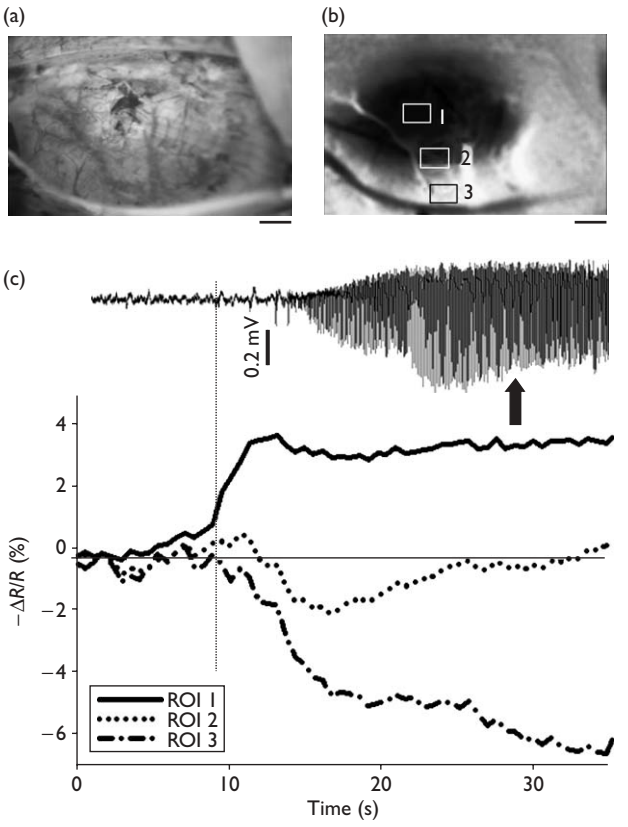

Fig. 2 (a) Image at 546 nm. Scale bar: 1 mm. (b) Divided image at 605 nm at time point indicated by vertical arrow in (c). Labels indicate regions of interest (ROIs) whose $-\Delta R/R$ (%) is shown in (c).

equilibrated with bubbling air (atmospheric pO_2) or 100% N_2 gas (zero pO_2). The O_2 microsensor was inserted 200–400 μm deep into the neocortex using a micromanipulator. The signal was measured with a PA 2000 picoammeter (Unisense A/S). Both pO_2 data and local field potential were recorded simultaneously onto a PC. Tissue oxygenation data were converted to percentage change from baseline by dividing the baseline value averaged over a 10 s block beginning 20 s before the onset of the ictal discharge. Statistical significance was determined with a paired *t*-test comparing the baseline mean (±SD) with the mean (±SD) tissue oxygenation at each time point.

Results

Sixty-seven seizures were imaged in six rats (15–21 seizures at each wavelength). After 4-AP injection, spontaneous seizures occurred periodically for up to 3 h with a mean (±SD) duration of 274.3±128.3 s and an interseizure interval of 5–20 min. Field potential recordings during seizures often exhibited transitions, such as those illustrated in Fig. 1b, from small amplitude, fast oscillations, reminiscent of low voltage fast activity, to a spike-and-wave pattern; such transitions have also been observed in human epilepsy [15,16].

A drop in light reflectance corresponded with the electrographic onset of each seizure (Fig. 1). Note that, as it is derived from slowly varying physiological changes in the neocortical tissue, the IOS is incapable of resolving subtle variations in the electrophysiology arising after seizure onset, such as the change in field potential frequency and amplitude between camera frames 14 and 16 in Fig. 1b.

We found no statistically significant change in IOS area, or in rate of seizure spread, as a function of wavelength. A trend was observed for imaging larger areas of spread at shorter wavelengths between 2 and 6 s after seizure onset, but did not rise to the level of statistical significance.

In all seizures, the time course of IOS within the focus was nearly monophasic and lasted throughout the duration of the seizure, indicating not only a persistent increase in CBV at the focus, but also a persistent increase in Hbr, consistent with a lengthy dip in oxygenation throughout the entire course of the ictal event, in spite of the increase in CBV at the focus. In all seizures imaged with orange light, and most of those imaged with green, a persistent increase in reflectance was observed at the seizure periphery, indicating a decrease in CBV and also a decrease in Hbr (increase in HbO_2). A typical decrease in Hbr (drop in reflectance) at the focus (ROI_1) and concomitant Hbr increase (increase in reflectance) in the surround (ROI_3) are shown in Fig. 2.

As the IOS measured at 605 and 630 nm is not a pure measure of Hbr, confirmation of the optical data was achieved with direct measurement of tissue oxygenation at the seizure focus with a Clark-style polarographic oxygen microsensor. In a separate group of three animals, seizure onset and duration (n=9) was accompanied by a long-lasting decrease in tissue oxygenation (Fig. 3). An average of all seizures (n=9), time locked to the seizure onset, showed a mean (SD) decrease in tissue pO_2 of 64.3±23.5% of baseline with a nadir at 24 s after seizure onset. The decrease in tissue pO_2 was statistically significant 5–35 s, and 45–50 s, after seizure onset (Fig. 3b).

Discussion

An increase in HbO_2 underlies the BOLD fMRI signal. Using the IOS, high-Tesla fMRI, oxygen-sensitive electrodes, and oxygen-dependent phosphorescence quenching, even more focal early decreases in blood oxygenation have been identified in the first few hundred milliseconds after normal sensory activation of the cortex [1,4,17–19]. This so-called 'initial dip' is considered to be more closely spatially linked to the population of active neurons than the later hyperoxygenation phase of the BOLD signal, which often arises from nearby draining veins, rather than metabolically active brain parenchyma [6,20].

Some investigators have questioned the initial dip's existence, as it is not observed under certain experimental conditions, and is highly dependent on anesthesia and oxygen saturation levels [17]. An explanation for erratic presence of a dip may be that its magnitude varies with the degree of cortical activation. Indeed, varying degrees of peripheral stimulation elicit graded dips in oxygenation [3,18].

Autoradiographic studies in various epilepsy models demonstrate 200–300% increases in oxygen metabolism [21]. Whether this increase is met with adequate CBF to prevent localized ischemia has been widely debated. Autoradiographic studies show that increased metabolic activity associated with status epilepticus is larger and more sustained than increased CBF [21], but the temporal resolution of autoradiography is extremely poor and the

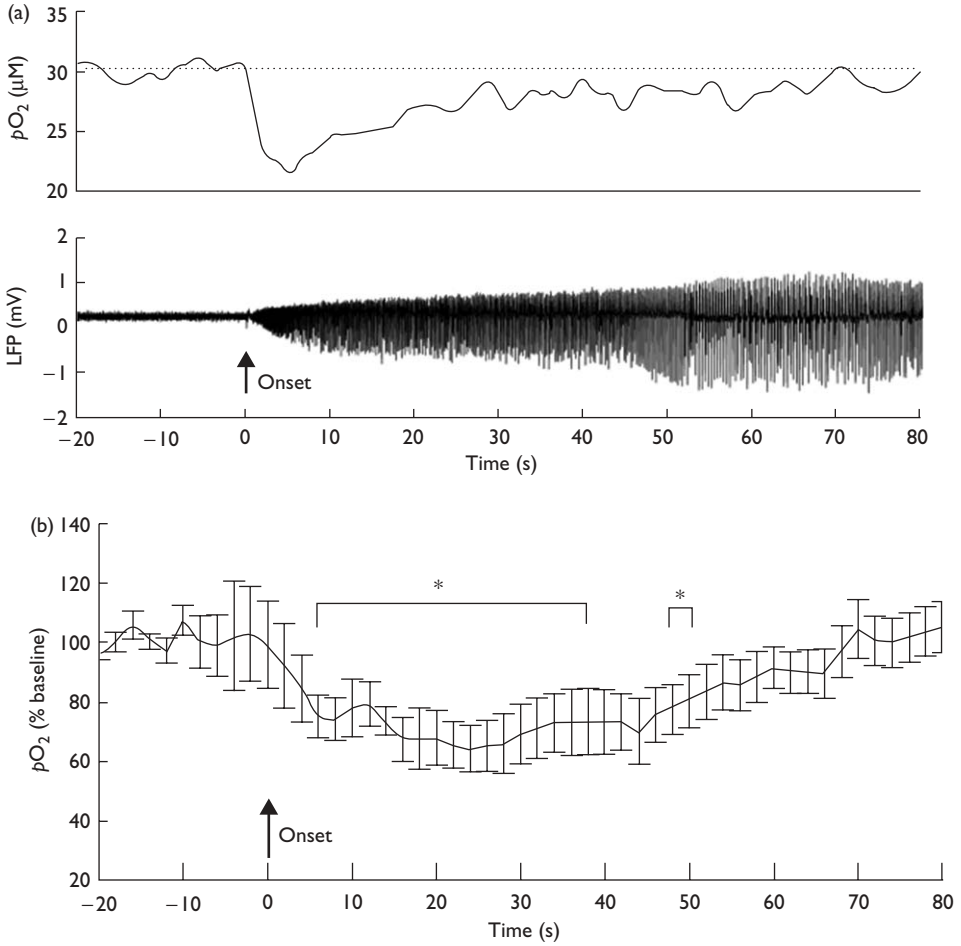

Fig. 3 (a) pO_2 (top trace) and local field potential (LFP, bottom trace) from a single animal. Arrow indicates the seizure onset; dashed line shows baseline tissue pO_2. (b) Mean (SE) percentage change in tissue pO_2 during ictal discharges (nine seizures in three rats, $*P < 0.05$).

relevance of this finding to interictal spikes or shorter duration seizures is unclear. Studies with fMRI, on epileptic events of shorter duration, showed that CBF oversupplies the focus with oxygenated blood [22]. Once again, the temporal resolution of fMRI is on the order of seconds rather than milliseconds and the spatial resolution on the order of millimeters rather than micrometers. In contrast, a recent IOS study showed a rapid drop in hemoglobin oxygenation after brief epileptiform events; this could not have been observed using lower temporal resolution techniques such as positron emission tomography, autoradiography or fMRI [10]. Here, we show that ictal events can elicit an even more profound increase in Hbr persisting for the entire length of the event.

Although the IOS at 605–630 nm is more sensitive to Hbr than HbO_2, it is possible that large changes in CBV (or Hbt) might influence the signal in the absence of a change in Hbr. For this reason, we directly measured tissue oxygenation, using an oxygen-sensitive electrode, and confirmed a rapid decrease in oxygenation at the onset of the seizure followed by a gradual drift back toward baseline (Fig. 3).

In contrast to the reflectance drop at the focus, we found an increase in reflectance in the brain surrounding the seizure. The significance of the 'inverted' IOS surrounding the epileptic focus has been debated. First described by Haglund *et al.* [9] at 690 nm after electrically triggered afterdischarges in the human cortex, it was attributed to 'shunting of blood' from the adjacent brain to the epileptic focus, although these authors recorded wavelengths sensitive to light scattering. At 707 nm, Schwartz and Bonhoeffer [8] found a similar inverted signal around an acute interictal spike focus in the ferret, correlating spatially with a decrease in the firing of extracellularly recorded neurons, and postulated that the inverted signal represented an 'inhibitory surround'. Supporting this theory, a reflectance increase following IOS mapping of functional architecture has been reported to coincide with a decrease in firing of extracellularly recorded neurons [23] and linked with neuronal inhibition [24].

We observe both a decrease in CBV in the surround and a profound decrease in Hbr (increase in HbO_2). Decreases in ictal surround perfusion, identified with Single Photon Emission Computed Tomography (SPECT) scanning in human patients, corroborates this peri-ictal CBV decrease [25]. One possible explanation for an HbO_2 increase in the surrounding parenchyma, despite a CBV decrease, is that neuronal inhibition reduces metabolic demand out of proportion with the shunting of blood to the focus.

Conclusions

Using IOS imaging of acute, focal seizures in the rat neocortex, and direct measurements with an oxygen-sensitive probe, we find a prolonged drop in oxygenation at the seizure focus. This finding indicates that, during the course of a seizure, an event that places a massive strain on the metabolic resources of the cortex, it is possible for the demand for oxygenated hemoglobin to exceed supply.

Acknowledgements

We gratefully acknowledge Koon-Ho Danny Wong for technical assistance, Dr Jonathan Victor for reading the manuscript, and Drs Irene Hueter, Anna Roe, and Benjamin M. Ramsden for a discussion of the statistical methods.

References

1. Frostig RD, Lieke EE, Ts'o DY, Grinvald A. Cortical functional architecture and local coupling between neuronal activity and the microcirculation revealed by in vivo high-resolution optical imaging of intrinsic signals. *Proc Natl Acad Sci USA* 1990; **87**:6082–6086.
2. Mayhew JEW, Johnston D, Berwick J, Jones M, Coffey P, Zheng Y. Spectroscopic analysis of neural activity in brain: increased oxygen consumption following activation of barrel cortex. *Neuroimage* 2000; **12**:664–675.
3. Nemoto M, Sheth S, Guiou M, Pouratian N, Chen JWY, Toga AW. Functional signal- and paradigm-dependent linear relationships between synaptic activity and hemodynamic responses in rat somatosensory cortex. *J Neurosci* 2004; **24**:3850–3861.
4. Malonek D, Grinvald A. Interactions between electrical activity and cortical microcirculation revealed by imaging spectroscopy: implications for functional brain mapping. *Science* 1996; **272**:551–554.
5. Sato K, Nariai T, Sasaki S, Yazawa I, Mochida H, Miyakawa N, *et al.* Intraoperative intrinsic signal imaging of neuronal activity from subdivisions of the human primary somatosensory cortex. *Cereb Cortex* 2002; **12**:269–280.
6. Cannestra AF, Pouratian N, Bookheimer SY, Martin NA, Becker DP, Toga AW. Temporal spatial differences observed by functional MRI and human intraoperative optical imaging. *Cereb Cortex* 2001; **11**:773–782.
7. Chen JWY, O'Farrell AM, Toga AW. Optical intrinsic signal imaging in a rodent seizure model. *Neurology* 2000; **55**:312–315.
8. Schwartz TH, Bonhoeffer T. In vivo optical mapping of epileptic foci and surround inhibition in ferret cerebral cortex. *Nature Med* 2000; **7**: 1063–1067.
9. Haglund MM, Ojemann GA, Hochman DW. Optical imaging of epileptiform and functional activity in human cerebral cortex. *Nature* 1992; **358**:668–671.
10. Suh M, Bahar S, Mehta AD, Schwartz TH. Temporal dependence in uncoupling of blood volume and oxygenation during interictal epileptiform events in rat neocortex. *J Neurosci* 2005; **25**:68–77.
11. Yang X-F, Duffy DW, Morley RE, Rothman SM. Neocortical seizure termination by focal cooling: temperature dependence and automated seizure detection. *Epilepsia* 2002; **43**:240–254.
12. Chen-Bee CH, Kwon MC, Masino SA, Frostig RD. Areal extent quantification of functional representations using intrinsic signal optical imaging. *J Neurosci Methods* 1996; **68**:27–37.
13. Lindauer U, Royl G, Leithner C, Kuhl M, Gold L, Gethman J, *et al.* No evidence for early decrease in blood oxygenation in rat whisker cortex in response to functional activation. *Neuroimage* 2001; **13**:988–1001.
14. Kohl M, Lindauer U, Royl G, Kuhl M, Gold L, Villringer A, *et al.* Physical model for the spectroscopic analysis of cortical intrinsic optical signals. *Phys Med Biol* 2000; **45**:3749–3764.
15. Kutsy RL, Farrell DF, Ojemann GA. Ictal patterns of neocortical seizures monitored with intracranial electrodes: correlation with surgical outcome. *Epilepsia* 1999; **30**:257–266.
16. Lee S-A, Spencer DD, Spencer SS. Intracranial EEG seizure-onset patterns in neocortical epilepsy. *Epilepsia* 2000; **41**:297–307.
17. Logothetis NK, Gugenberger H, Peled S, Pauls J. Functional imaging of the monkey brain. *Nat Neurosci* 1999; **2**:555–562.
18. Thompson JK, Peterson MR, Freeman RD. Single-neuron activity and tissue oxygenation in the cerebral cortex. *Science* 2003; **299**:1070–1072.
19. Vanzetta I, Grinvald A. Increased cortical oxidative metabolism due to sensory stimulation: implications for functional brain imaging. *Science* 1999; **286**:1555–1558.
20. Vanzetta I, Grinvald A. Evidence and lack of evidence for the initial dip in the anesthetized rat: implications for human functional brain imaging. *Neuroimage* 2001; **13**:959–967.
21. PeiradeVasconcelos A, Ferrandon A, Nehlig A. Local cerebral blood flow during lithium-pilocarpine seizures in the developing and adult rat: role of coupling between blood flow and metabolism in the genesis of neuronal damage. *J Cereb Blood Flow Metab* 2002; **22**:196–205.
22. Benar C-G, Gross DW, Wang Y, Petre V, Pike B, Dubeau F, *et al.* The BOLD response to interictal epileptiform discharges. *Neuroimage* 2002; **17**:1182–1192.
23. Schuett S, Bonhoeffer T, Hubener M. Mapping retinotopic structure in mouse visual cortex with optical imaging. *J Neurosci* 2002; **22**:6549–6559.
24. Das A, Gilbert CD. Long-range horizontal connections and their role in cortical reorganization revealed by optical recording of cat primary visual cortex. *Nature* 1995; **375**:780–784.
25. Van Paesschen W, Dupont P, Van Driel G, Van Billoen H, Maes A. SPECT perfusion changes during complex partial seizures in patients with hippocampal sclerosis. *Brain* 2003; **126**:1103–1111.